International Journal of Mass Spectrometry 278 (2008) 50–58

Contents lists available at ScienceDirect

International Journal of Mass Spectrometry

journal homepage: www.elsevier.com/locate/ijms

Dissociation of bromo- and iodotoluene molecular ions: A theoretical study

Joong Chul Choe*

Department of Chemistry, Dongguk University, 3-26 Pil-dong, Chung-gu, Seoul 100-715, Republic of Korea

ARTICLE INFO

Article history:
Received 12 June 2008
Received in revised form 28 July 2008
Accepted 7 August 2008
Available online 15 August 2008

Keywords:
Benzylium
Tropylium
Tolylium
DFT calculation
RRKM calculation

ABSTRACT

The potential energy surfaces (PESs) for the formation of $C_7H_7^+$ from α-, *o*-, *m*-, and *p*-halotoluene (X = Br and I) molecular ions were determined using density functional theory molecular orbital calculations. Based on the PESs, Rice–Ramsperger–Kassel–Marcus model calculations were carried out to predict the dissociation rate constants of the molecular ions, which were then compared with previous experimental results. Kinetic analysis showed that below the threshold for the formation of tolylium ion (Tl^+), the benzylium ion (Bz^+) was the main product in the dissociation of all molecular ions investigated. The α-halotoluene ions produced Bz^+ by direct C–X bond cleavage. The formation of Bz^+ from *o*-halotoluene ions occurred mainly through isomerization to the alpha isomers. On the other hand, the halogenated isotoluene ions played important roles as intermediates in the formation of Bz^+ from the *meta* and *para* isomers. The formation of Tl^+ became important as the energy increases in the dissociations of *o*-, *m*-, and *p*-halotoluene ions, especially in those of *o*-, *m*-iodotoluene ions.

1. Introduction

Several studies have examined the formation of $C_7H_7^+$ from toluene molecular ion and its derivatives in the gas phase using a variety of experimental and theoretical methods [1–36]. Since Rylander et al. [1] first proposed the tropylium ion (Tr^+) as a $C_7H_7^+$ product formed through the ionization of toluene and ethylbenzene, the structural identification of $C_7H_7^+$ products has been a major focus in studies of the dissociation of numerous molecular ions of toluene derivatives including halo substituted toluenes. It is well known that both the benzylium ion (Bz^+) and Tr^+ are produced from the toluene ion through direct C–H bond cleavage and ring expansion, respectively [2,3]. Ring expansion begins with a 1,2-shift of an H atom of the methyl group to form a distonic benzenium ion (**b**), and the cycloheptatriene ion (**d**) is formed via the norcaradiene ion (**c**) (Scheme 1) through a process known as the Hoffman mechanism [4]. Recently, it was reported that the loss of H• by a rearrangement to *o*-isotoluene (5-methylene-1,3-cycloheptadiene) ion (**e**) is another competitive dissociation channel [5]. A previous study of isomeric xylene ions reported that the pathways via methyl substituted isotoluene ions play a very important role in the formation of Bz^+ [6].

Various experimental methods have been employed to examine the dissociation of halotoluene ions [7–16,18–22]. The dissociation rate constants of chloro-, bromo-, and iodotoluene ions were measured using a photoelectron-photoion coincidence (PEPICO) method [7]. Those of bromo- and/or iodotoluene ions were measured using a time-resolved photodissociation (TRPD) method, based on Fourier transform ion cyclotron resonance (FT-ICR) spectrometry [9–13], and photodissociation using mass-analyzed ion kinetic energy spectrometry (PD-MIKES) [15,16]. In PD-ICR studies for isomeric bromo- and iodotoluene ions, Shin and co-workers reported that Bz^+ is produced exclusively below the thresholds of the formation of tolylium ion (Tl^+) [9–12]. They suggested that the dissociation pathway to Bz^+ through halogenated isotoluene ions would be favored kinetically over the pathway to Tr^+, via ring expansion.

Recently, the potential energy surface (PES) for the isomerization and dissociation of α-, *o*-, *m*-, and *p*-chlorotoluene ions was explored using molecular orbital (MO) calculations [17]. The kinetic analysis by Rice–Ramsperger–Kassel–Marcus (RRKM) [37] model calculations predicted that the only $C_7H_7^+$ product is Bz^+, which is formed mainly via chlorinated isotoluene ions. This study examined the dissociation kinetics of isomeric bromo- and iodotoluene molecular ions theoretically using the same method. As in the dissociation of chlorotoluene ions, it was predicted that below the threshold for Tl^+ formation, Bz^+ would be the main $C_7H_7^+$ product formed by rearrangements. The main dissociation pathways for iodotoluene ions were different from those of the chlorine and bromine analogues. This paper discusses the similarity and difference in the reactions of substituted toluene ions.

* Tel.: +82 2 2260 8914; fax: +82 2 2268 8204.
E-mail address: jcchoe@dongguk.edu.

1387-3806/$ – see front matter © 2008 Elsevier B.V. All rights reserved.
doi:10.1016/j.ijms.2008.08.003

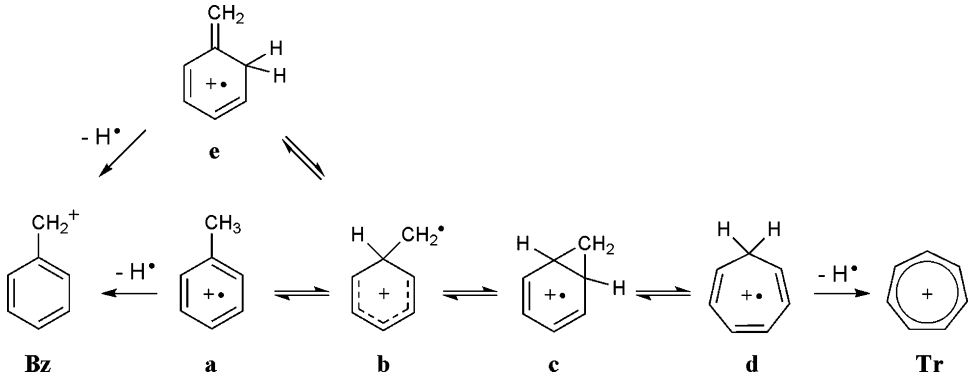

Scheme 1.

2. Computational methods

The MO calculations were performed using the Gaussian 03 suite of programs [38]. Geometry optimizations for the stationary points were carried out at the unrestricted B3LYP level of density functional theory (DFT). The 6-311G(d,p) basis set was used for C and H atoms and the Stuttgart/Dresden (SDD) relativistic effective core potential (ECP) basis set [39] was used for Br and I atoms. The transition state (TS) geometries connecting the stationary points were searched and checked by calculating the intrinsic reaction coordinates (IRCs) at the same level.

The RRKM expression was used to calculate the rate-energy dependences as follows [37]:

$$k(E) = \frac{\sigma N^{\neq}(E - E_0)}{h\rho(E)}, \quad (1)$$

where E is the reactant internal energy, E_0 the critical energy of the reaction, $N^{\neq}$ the sum of the TS states, ρ the density of the reactant states, and σ is the reaction path degeneracy. $N^{\neq}$ and ρ were evaluated by a direct count of the states using the Beyer–Swinehart algorithm [40].

3. Results and discussion

3.1. Isomerization and dissociation pathways

For the bromo- and iodotoluene molecular ions, the reaction pathways obtained were parallel. Scheme 2 shows the isomerization and dissociation pathways of the α-, *o*-, *m*-, and *p*-halotoluene (X = Br and I) ions (**1a**, **2a**, **3a**, and **4a**, respectively) obtained using the DFT calculations. The energies of the stable species and the TSs connecting them relative to **2a** are also included in the scheme. Figs. 1 and 2 show the potential energy diagrams for the reactions of the isomeric bromo- and iodotoluene ions, respectively. **1a** can produce Bz^+ by direct C–X bond cleavage or Tr^+ by a rearrangement to the seven-membered ring isomer, **1d** (the Hoffman mechanism) followed by the loss of X•. The rearrangement begins with a 1,2-shift of an H atom of the CH_2X group. Alternatively, the X atom can migrate to the *ipso* carbon with ring closure to form a halogenated norcaradiene ion (**2c**). According to the IRC calculation, when an X atom bonded to C1 (the labeling for each C atom is shown in Fig. 3) shifts toward C2, the CH_2 group moves away from X, and the C1–C2 bond moves out from the plane of the benzene ring. After passing the TS, which is designated by **B1a2c** or **I1a2c** (**B** and **I** stand for the bromo- and iodo-substitutions, respectively), the CH_2 group moves toward C3 as the C2–X distance decreases, and forms the C1–C2–C3 three-membered ring. This rearrangement is less favored than the 1,2-H shift due to its higher barrier height. Reverse isomerization, **2c** → **1a**, can play an important role in the dissociation of **2a**, as described below. Analogous pathway was found in the reaction of α-chlorotoluene ion [17], even though there are few reports of such rearrangements by a halogen shift [41–43]. However, these two types of rearrangements by the Hoffman mechanism cannot compete with the direct loss of X• in the formation of Bz^+ due to their higher barriers.

Each of **3a** and **4a** can also undergo ring expansion through the Hoffman mechanism. In the reactions of **2a**, it was found that **2b** isomerized to **2c** through a two-step mechanism via **3c**, which is similar to the mechanisms reported for the reactions of *o*-xylene [6] and *o*-chlorotoluene [17] ions. The four seven-membered ring isomers (**1d**–**4d**) are interconvertible by an "H-ring walk". The halogenated norcaradiene ions (**2c**–**4c**) can interconvert by a "CH_2-ring walk".

Each of the distonic benzenium ions (**1b**–**4b**) can undergo an H-ring walk, as shown in Scheme 2b. Among the halogenated isotoluene ions formed by such rearrangements, those (**2i** and **4g**), where the X and H atoms are bonded to the same C atom can produce Bz^+ through the loss of X•. The other isomer that can produce Bz^+ easily, **3h** (see Scheme 2b), was not optimized. It should be noted that **3h** would be much more unstable than **2i** or **4g** due to lack of conjugated double bonds. A previous study on chlorotoluene ions [17] reported that all three analogous isotoluene ions that can produce Bz^+ were optimized. The reported energies of **C3h** and **C4g** are 63 and 15 kJ mol^{-1} higher than **C2i**, respectively (these abbreviations are used for the chlorine analogues). Instead, **3g** and **3i** can lose X• to produce Bz^+ after surmounting a TS for the 1,2-H shift.

2a–**4a** can produce *o*-, *m*-, and *p*-tolylium ions (oTl^+, mTl^+, and pTl^+, respectively), respectively through direct C–X bond cleavage. Their TSs were not located, indicating that the dissociations occurred without reverse barriers.

3.2. RRKM model calculations

The present MO calculations showed that the dissociations starting from the α isomers of the halotoluene ions produced Bz^+ exclusively through the loss of X•. For the *ortho*, *meta*, and *para* isomers, the energy barriers for the formation of Bz^+ are lower than those of Tr^+ (Figs. 1 and 2), which also suggests the favored formation of Bz^+. However, since the energy barriers are similar, the detailed dissociation kinetics cannot be predicted using an energetic factor only. In order to estimate the contributions of the individual pathways to the formation of $C_7H_7^+$ from the *ortho*, *meta*, and *para* isomers, RRKM model calculations were carried out based on the theoretical PESs. The overall dissociation rate constants obtained were compared with the previous experimental data.

Because the PESs for the dissociations by several rearrangements obtained are quite complicated, the rate constants of

the individual reaction channels to produce Bz^+ and Tr^+ were estimated using a few approximations. First, some intermediates were treated as a common intermediate, which will be called an intermediate group (IG) here, because they interconvert rapidly prior to further reactions. Scheme 3 shows the approximated isomerization and dissociation pathways of **2a** including the five IGs. The reactions starting from **2a** were categorized by seven parallel channels consisting of four Bz^+ formations, one Tr^+ formation, and isomerizations to **3a** and **4a**. For the reactions from **3a** or **4a**, the approximated reaction pathways are similar to those in Scheme 3. There are seven reaction channels of **3a**; channel 3a_Bz1: **3a** ⇌ **3b** → IG1 → **1a** → $Bz^+ + X^•$, channel 3a_Bz2: **3a** ⇌ **3b** → IG1 → IG2 → $Bz^+ + X^•$, channel 3a_Bz3: **3a** ⇌ **3b** → IG5 → $Bz^+ + X^•$ (including **3b** → **3i** → $Bz^+ + X^•$), channel 3a_Bz4: **3a** ⇌ **3b** → IG3 → IG4 → $Bz^+ + X^•$, channel 3a_Tr: **3a** ⇌ **3b** → IG1 → $Tr^+ + X^•$, channel 3a_2a: **3a** ⇌ **3b** → IG1 → **2a**, channel 3a_4a: **3a** ⇌ **3b** → IG3 → **4a**. There are seven reaction channels of **4a**; channel 4a_Bz1: **4a** ⇌ IG3 → IG1 → **1a** → $Bz^+ + X^•$, channel 4a_Bz2: **4a** ⇌ IG3 → IG1 → IG2 → $Bz^+ + X^•$, channel 4a_Bz3: **4a** ⇌ IG3 → **3b** → IG5 → $Bz^+ + X^•$ (including **3b** → **3i** → $Bz^+ + X^•$), channel 4a_Bz4: **4a** ⇌ IG3 → IG4 → $Bz^+ + X^•$, channel 4a_Tr: **4a** ⇌ IG3 → IG1 → $Tr^+ + X^•$, channel 4a_2a: **4a** ⇌ IG3 → IG1 → **2a**, channel 4a_3a: **4a** ⇌ IG3 → **3b** → **3a**. In addition, IG3 can isomerize to IG1 through **3b**.

Second, the steady-state approximation can be used because the starting molecular ions, the *ortho*, *meta*, and *para* isomers, are much more stable than all the intermediates, which means that the reactions occurring from the intermediates are much faster than the first step of the dissociation (for example, **B2a** → **B2b** in the dissociation of **B2a**). Consider a reaction that produces several products, P_is from reactant A, through a common intermediate, B, with a very short lifetime:

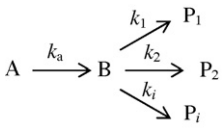

(2)

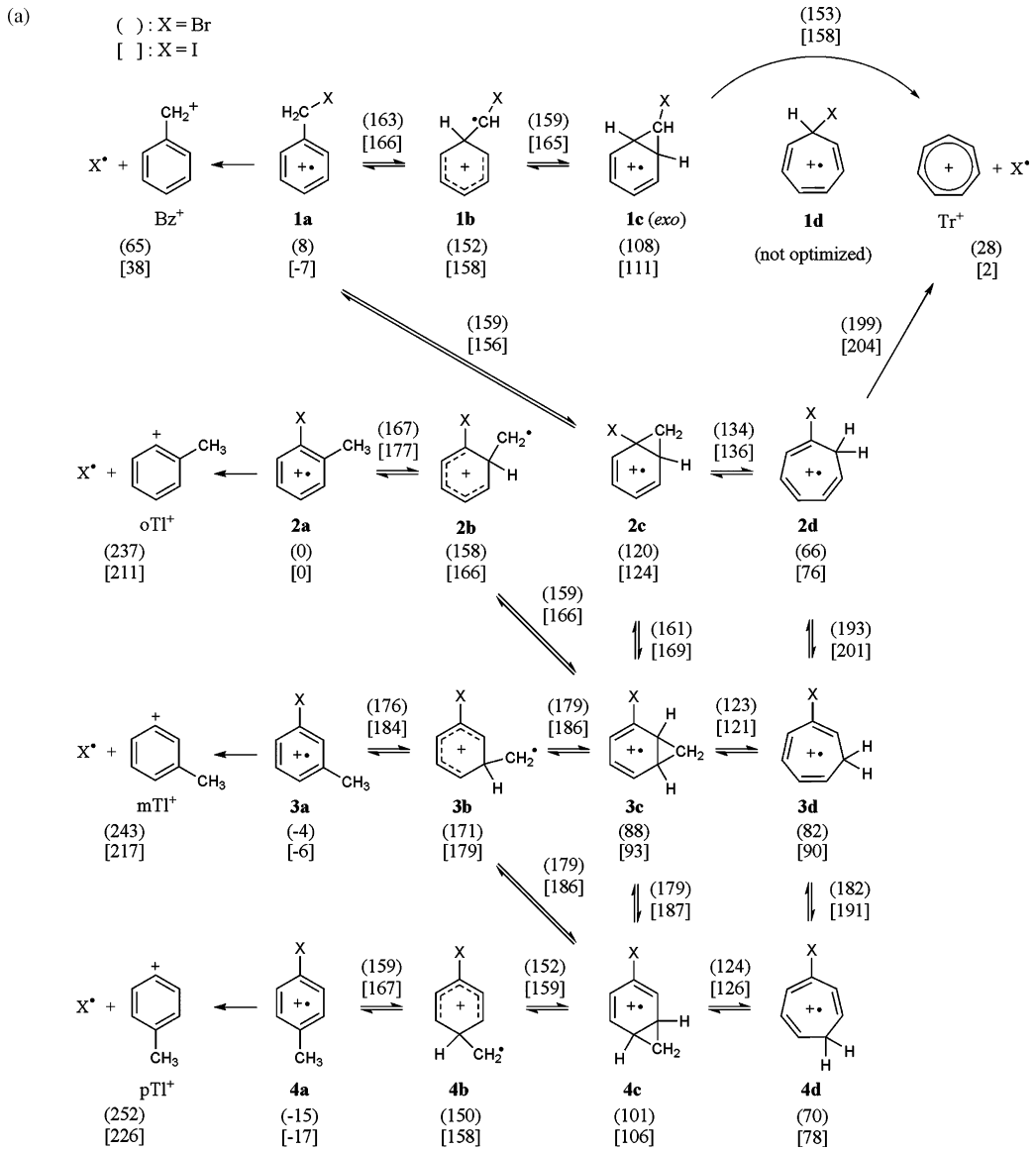

Scheme 2. The isomerization and dissociation pathways of (a) **1a**–**4a** and (b) **1b**–**4b** obtained by B3LYP/6-311G(d,p)(C,H)/SDD(Br,I) calculations. The relative energies (in kJ mol^{-1}) are shown in the parentheses and brackets for the bromo- and iodotoluene ions, respectively. The values next to the arrows are for TSs. The ZPVE corrections are included.

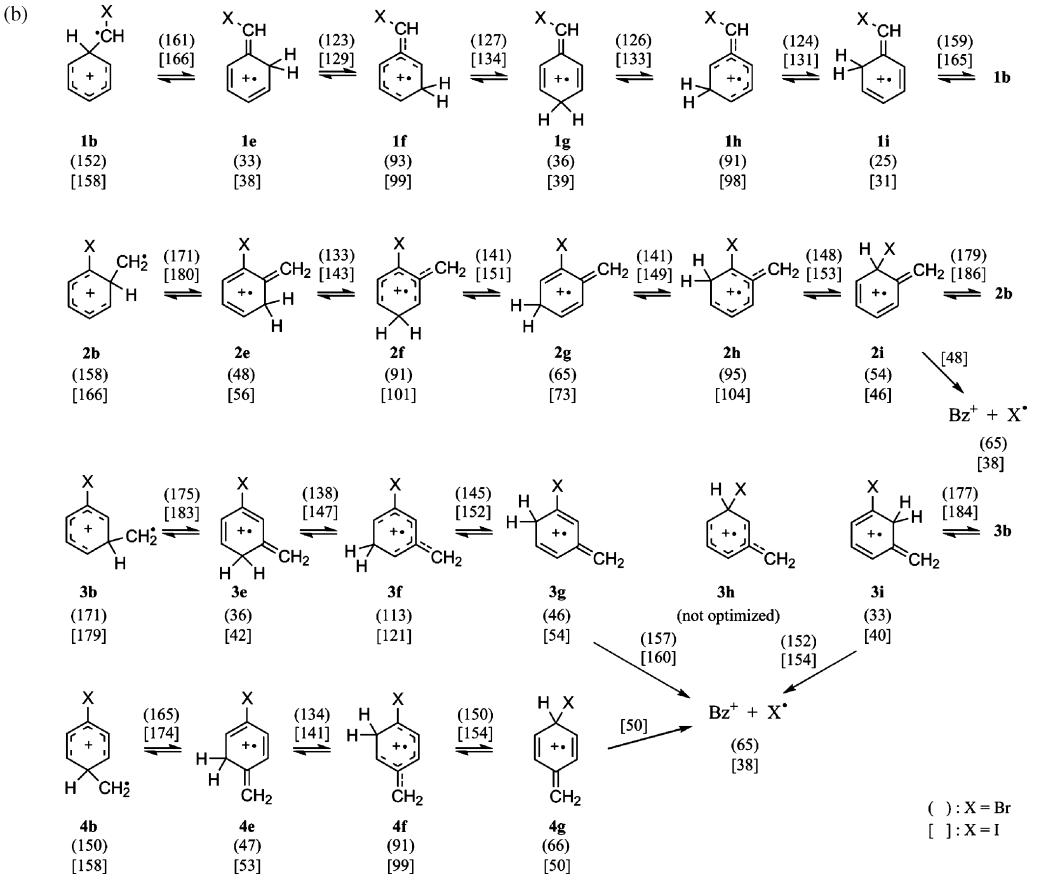

Scheme 2. (*Continued*).

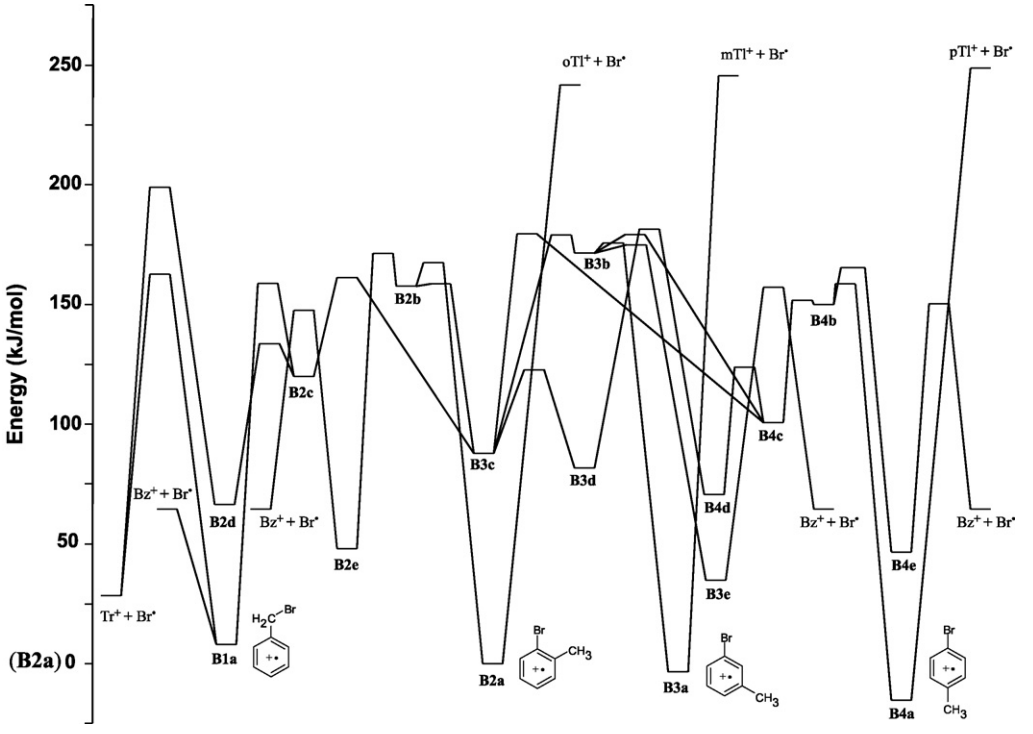

Fig. 1. Potential energy diagram for the isomerization and dissociation of the bromotoluene ions derived from the B3LYP calculations. For convenience, the isomerization pathways of **B2b**, **B3b**, and **B4b** to the several brominated isotoluene intermediates were approximated using one-well potentials, and the barriers to produce Tr^+ from **B1a** were approximated by one barrier. The pathway **B2d** → **B3d** and that through **B1e**–**B1i** are not included.

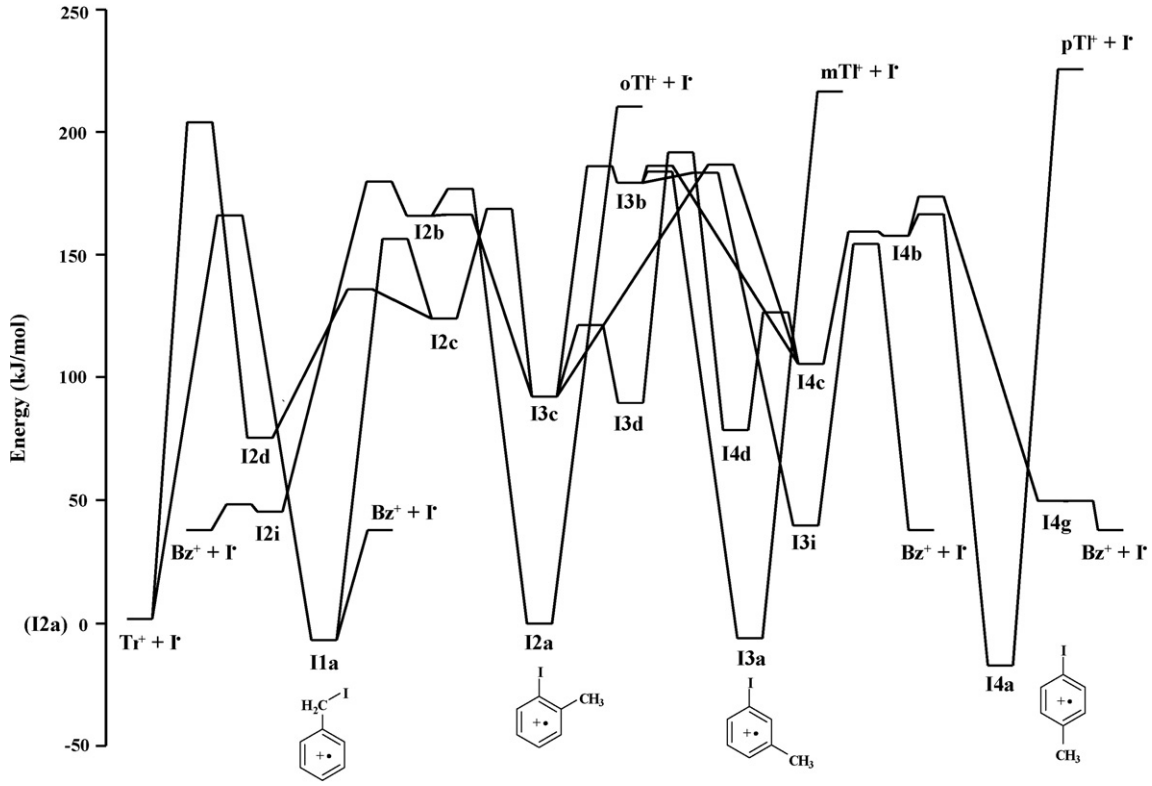

Fig. 2. Potential energy diagram for the isomerization and dissociation of the iodotoluene ions derived from the B3LYP calculations. For convenience, the isomerization pathways of **I2b**, **I3b**, and **I4b** to the several iodinated isotoluene intermediates were approximated using one-well potentials, and the barriers to produce Tr^+ from **I1a** were approximated by one barrier. The pathway **I2d** → **I3d** and that through **I1e**–**I1i** are not included.

With the steady-state approximation, the rate constant to produce P_i is determined by

$$k_{p,i} = k_a f_i. \tag{3}$$

where f_i is the fraction of the i channel given by

$$f_i = \frac{k_i}{\sum_i k_i}. \tag{4}$$

The overall rate constant is the sum of $k_{p,i}$s and the abundance of P_i is proportional to $k_{p,i}$. When the backward isomerization, B → A, is competitive to the forward reactions, its rate constant should be added to the sum in the denominator of Eq. (4). The reaction can be more complicated. When there is another pathway to form B from A, for example A → C → B, its rate constant should be added to k_a in Eq. (3). When an unstable P_i undergoes further parallel reactions to Q_js, the rate constant to produce Q_j is given by $k_a f_i f_j$, where f_j is the fraction of the j channel out of reactions from P_i.

Third, although some backward isomerization steps are competitive toward further reactions, only the first one (as IG1 → **2a** in Scheme 3) was considered. The errors that arise from this approximation were estimated to be a small proportion (a few percent) of the overall dissociation rate constants.

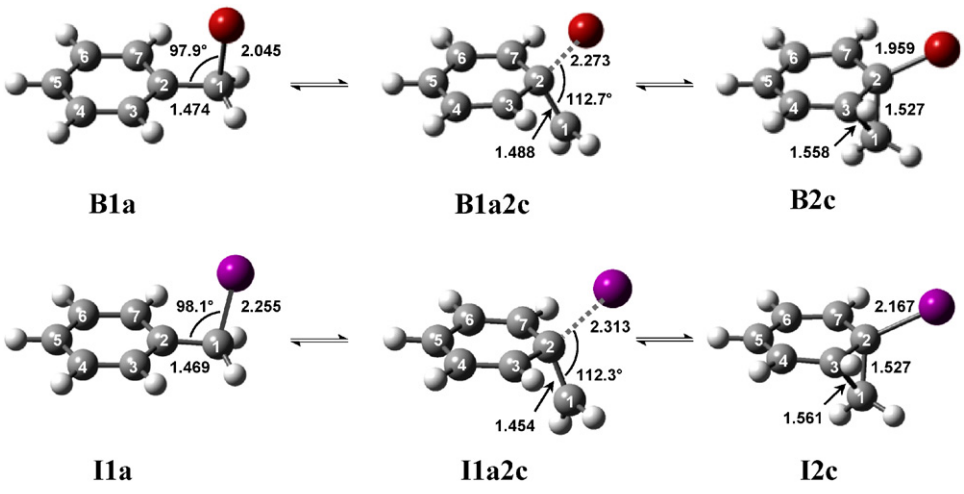

Fig. 3. Isomerization pathways of the *o*-bromo- and *o*-iodotoluene ions occurring by an X shift with the geometric structures optimized using the B3LYP calculations. The distances are in Å.

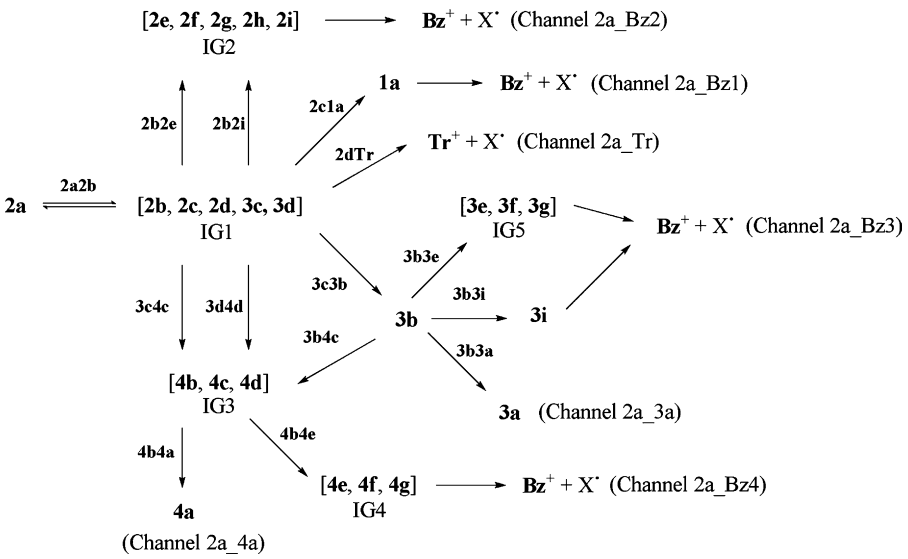

Scheme 3.

3.2.1. Iodotoluene ions

The experimental rate data for the dissociation of *m*-iodotoluene ion (**I3a**) are available on the time scales (ms–ns) wider than those (ms–μs) for the other molecular ions investigated here. Thus, the results for **I3a** will be described first. First of all, the rate constant (k_{Rearr}) for the dissociations by rearrangements was calculated using the above approximations. Secondly, the rate constant for the production of mTl^+ (channel I3a_mTl) occurring by direct C–I bond cleavage was considered. The overall dissociation constant is the sum of these two contributions.

According to the above second approximation, the rate constants of the individual channels by rearrangements were determined using the rate constant of the first step multiplied by their branching ratios (see Eq. (3)). The branching ratios were determined from the rate constants of the reactions of the intermediates relevant to the individual channels. In order to predict the reaction rate constants of **I3a**, the RRKM rate constants (Eq. (1)) were calculated for the individual steps with the TSs, as denoted next to the arrows in Scheme 3. The steps for which no TSs are indicated are the reactions occurring very fast, which do not affect the rate constants of the individual channels. The critical energies and vibrational frequencies obtained from the present DFT calculation were used in the RRKM calculation. The rate constants of the seven channels were obtained from these calculated individual rate constants. Fig. 4 shows the obtained rate-energy dependences. Channel I3a_Bz3 is the fastest among the channels by rearrangements, which produces Bz^+ through the isotoluene ions iodinated at the *meta* position and is the minimum energy reaction pathway (MERP) needed to produce $C_7H_7^+$ from **I3a**. The next important channels are I3a_Bz1, I3a_4a, and I3a_Bz4. The contributions from the others are small and the formation of Tr^+ (channel I3a_Tr) is negligible. k_{Rearr} is the sum of the five dissociation channels, I3a_Bz1, I3a_Bz2, I3a_Bz3, I3a_Bz4, and I3a_Tr, which is shown in Fig. 4. Comparing to experimental data, it closes to the ICR data, but underestimates the PD-MIKES data by an order of magnitude. This is due to ignoring channel I3a_mTl, occurring via a loose TS. Since the TS for the direct C–I bond cleavage was not located, its dissociation rate constant (k_{mTl}) will not be predicted using conventional RRKM calculations. Thus, to obtain the rate-energy dependence for the channel, the vibrational frequencies for the TS were adjusted so that the overall dissociation rate constants ($k_{Rearr} + k_{mTl}$) agree with the PD-MIKES experimental ones. In the RRKM calculation, the critical energy and vibrational frequencies for **I3a** obtained using DFT calculations were used, and the C–I stretch mode (695 cm^{-1}) was taken as the reaction coordinate. The rate-energy dependences in Fig. 4 show that at low energy the formation of Bz^+ is dominant, while as increasing energy the formation of mTl^+ becomes dominant, which agrees with the general tendency in competition between dissociations by rearrangement and direct bond cleavage.

The entropy of activation is ($\Delta S^{\ddagger}$) a good parameter characterizing the property of a TS [37]. The $\Delta S^{\ddagger}$ value calculated at 1000 K for the formation of mTl^+ was 36.0 J mol^{-1} K^{-1}, which indicates that the dissociation occurs by a loose TS and is comparable to that (31.2 J mol^{-1} K^{-1}) reported for the formation of phenyl ion by direct C–I bond cleavage of iodobenzene ion [44].

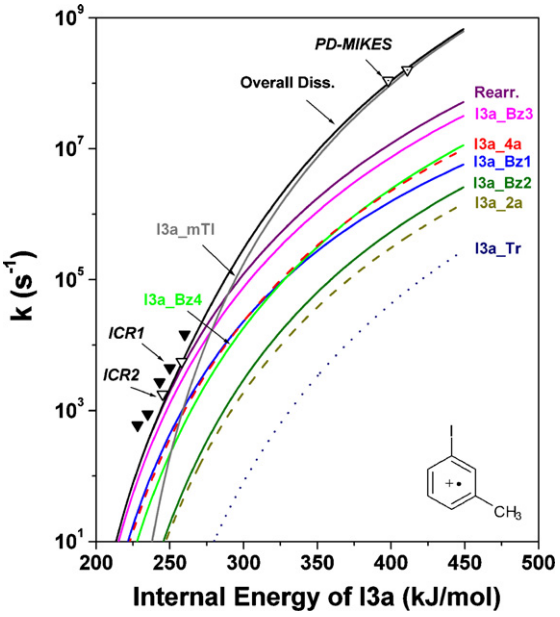

Fig. 4. Rate-energy dependences for the individual reaction channels, k_{Rearr}, and the overall dissociation of *m*-iodotoluene ion. The curves are the results of RRKM model calculations. The points are the experimental results by ICR1 [10], ICR2 [13] and PD-MIKES [15].

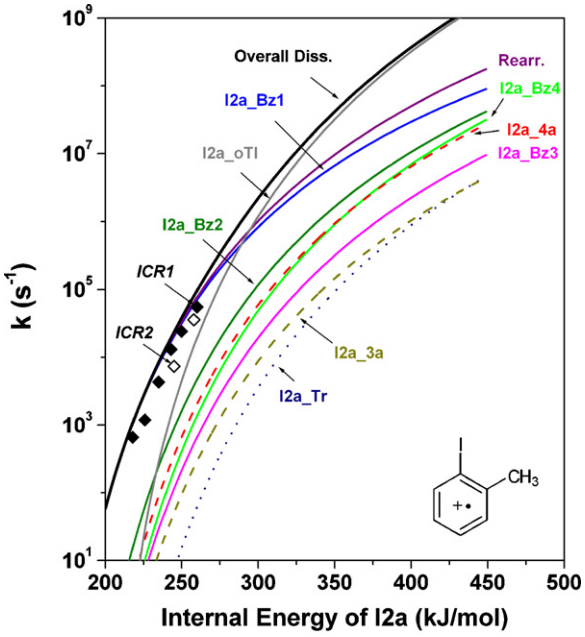

Fig. 5. Rate-energy dependences for the individual reaction channels, k_{Rearr}, and the overall dissociation of *o*-iodotoluene ion. The curves are the results of RRKM model calculations. The points are the experimental results by ICR1 [10] and ICR2 [13].

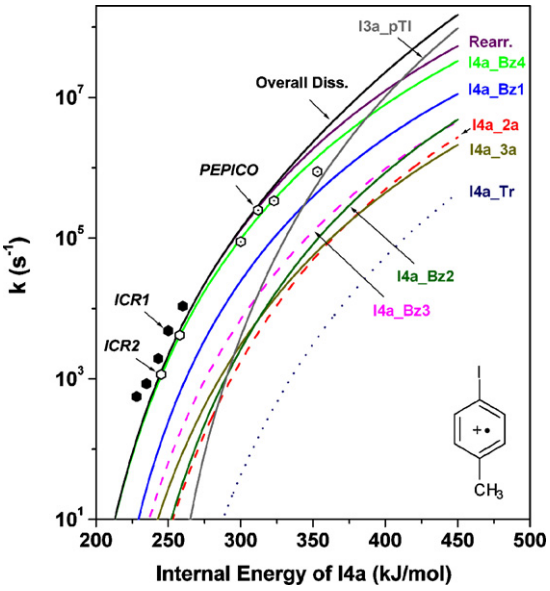

Fig. 6. Rate-energy dependences for the individual reaction channels, k_{Rearr}, and the overall dissociation of *p*-iodotoluene ion. The curves are the results of RRKM model calculations. The points are the experimental results by ICR1 [10], ICR2 [13] and PEPICO. The PEPICO data are the results reanalyzed by Lin and Dunbar [13] using the original data reported by Olesik et al. [7].

For the dissociations of *o*- and *p*-iodotoluene ions (**I2a** and **I4a**, respectively), k_{Rearr}'s were calculated the same way. To calculate the RRKM rate constants for the formation of oTl^+ (channel I2a_oTl, k_{oTl}) and pTl^+(channel I4a_mTl, k_{pTl}), it was assumed that the $\Delta S^{\ddagger}_{1000\,K}$ values are the same as that obtained above for k_{mTl}. The vibrational frequencies for the respective TSs were adjusted so that the $\Delta S^{\ddagger}_{1000\,K}$ values became 36.0 J mol^{-1} K^{-1}. The critical energies and vibrational frequencies for the reactants obtained by DFT calculations were used. Fig. 5 shows the RRKM rate constants for the individual rearrangement channels, k_{Rearr}, and k_{oTl} along with experimental data for the dissociation of **I2a**. The main dissociation channel by rearrangement is I2a_Bz1, which produces Bz^+ via **I1a** and is the MERP needed to produce $C_7H_7^+$ from **I2a**. The contributions from the other channels are negligible at low energies, but those from channels I2a_Bz2, I2a_Bz4, and I2a_4a become important as the energy increases. The formation of oTl^+ becomes dominant as the energy increases. The overall rates are close to the experimental data obtained on sub-microsecond time scales. Further rate experiments are needed on the shorter time scales to analyze the dissociation kinetics with better accuracy.

Fig. 6 shows the rate-energy dependences for the individual rearrangement channels along with those for k_{Rearr}, overall dissociation rate, and experimental ones for the dissociation of **I4a**. The most important dissociation channel by rearrangement is I4a_Bz4, which is the MERP needed to produce $C_7H_7^+$ from **I4a**. The contribution of channel I4a_Bz1 cannot be neglected. The others contribute to the dissociation negligibly. The contribution from the formation of pTl^+ is smaller than those in the dissociations of *o*- and *m*-iodotoluene. This is due to the relatively high critical energy for the formation pTl^+. The overall dissociation rate-energy dependence is close to the ICR and PEIPCO experimental data.

3.2.2. Bromotoluene ions

In the dissociations of bromotoluene ions, it is expected that the contributions from formation of Tl^+ are smaller than those of iodine analogues, because the products lie much higher than the barriers for rearrangements when comparing with the iodine analogues (Figs. 1 and 2). To estimate the contributions, the rate-energy dependences were calculated by assuming that the $\Delta S^{\ddagger}_{1000\,K}$ values were the same as that (33.8 J mol^{-1} K^{-1}) reported for the formation of phenyl ion by direct C–Br bond cleavage of bromobenzene ion [45].

Fig. 7 shows the theoretical and experimental rate-energy dependences for the dissociation of *o*-bromotoluene ion (**B2a**). Channel B2a_Bz1 is the most important dissociation channel by rearrangement, which is the MERP needed to produce $C_7H_7^+$ from **B2a**. The minor channels B2a_Bz2, B2a_4a, and B2a_Bz4 become

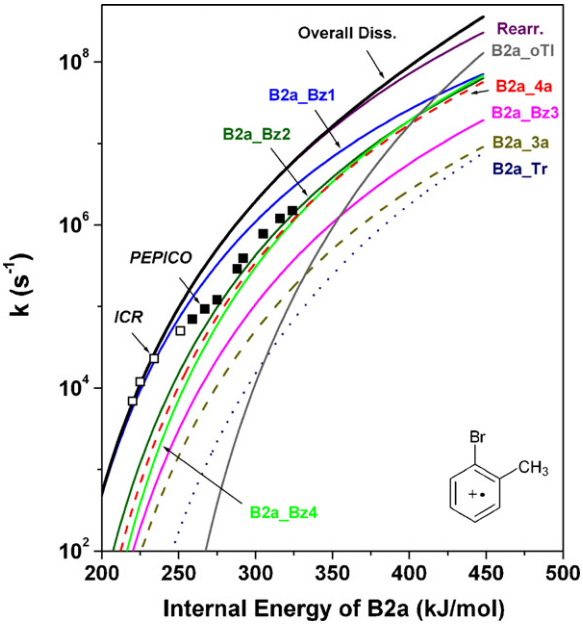

Fig. 7. Rate-energy dependences for the individual reaction channels, k_{Rearr}, and the overall dissociation of *o*-bromotoluene ion. The curves are the results of RRKM model calculations. The points are the experimental results by ICR [9] and PEPICO [7].

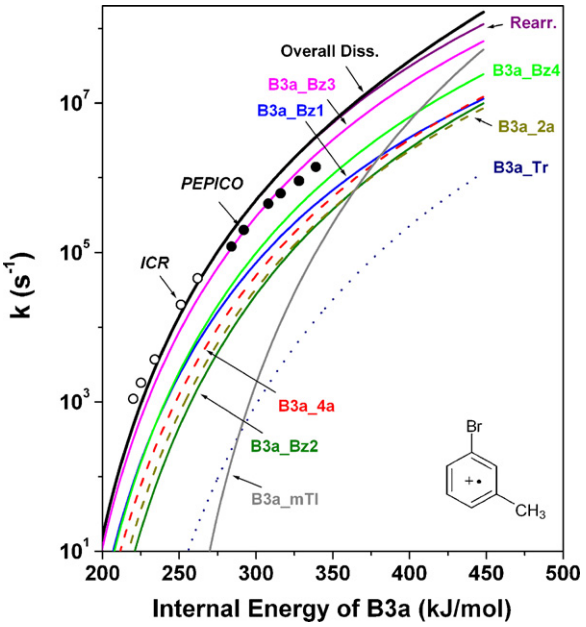

Fig. 8. Rate-energy dependences for the individual reaction channels, k_{Rearr}, and the overall dissociation of *m*-bromotoluene ion. The curves are the results of RRKM model calculations. The points are the experimental results by ICR [9] and PEPICO [7].

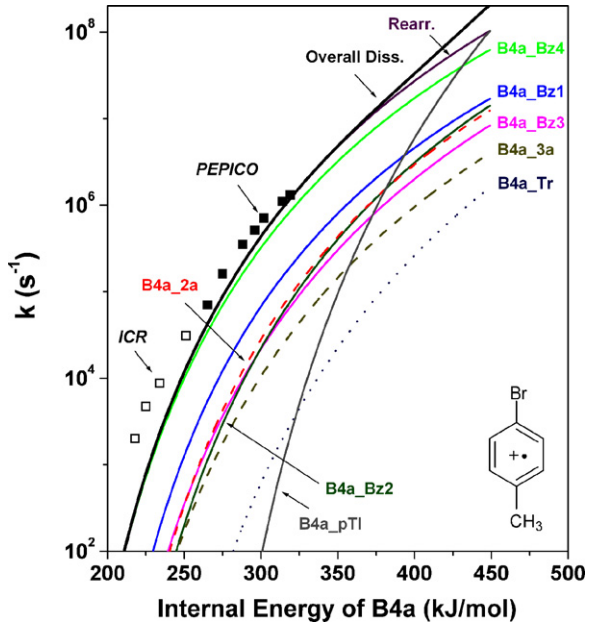

Fig. 9. Rate-energy dependences for the individual reaction channels k_{Rearr}, and the overall dissociation of *p*-bromotoluene ion. The curves are the results of RRKM model calculations. The points are the experimental results by ICR [9] and PEPICO [7].

important as increasing energy. The other channels contribute negligibly to the dissociations. Up to 350 kJ mol^{-1}, the contribution from formation of oTl$^+$ is negligible, and become important at higher energies. The overall dissociation rate constants agree well with the ICR data, but about three times larger than the PEPICO data.

Fig. 8 shows the theoretical and experimental rate-energy dependences for the dissociation of *m*-bromotoluene ion (**B3a**). Channel B3a_Bz3 is the main dissociation channel by rearrangement, which is the MERP needed to produce $C_7H_7^+$ from **B3a**. The other channels cannot be neglected, except the formation of Tr$^+$. The contribution from formation of mTl$^+$ is similar with the dissociation of **B2a**. The agreement between the overall dissociation rates and experimental ones is satisfactory.

The rate-energy dependences for the dissociation of *p*-bromotoluene ion (**B4a**) are shown in Fig. 9. Among the dissociation channels by rearrangement, B4a_Bz4 is the most important, which is the MERP needed to produce $C_7H_7^+$ from **B4a**. The contributions from the other channels are small. At high energy, the formation of pTl$^+$ can contribute to the dissociation. The overall dissociation rates close to the experimental data (Fig. 9).

For the *o*-, *m*-, and *p*-halotoluene ions investigated, the theoretical dissociation rates closed to the experimental ones, but did not predict exactly. This may be due to several reasons. The most probable one is limited accuracy of the energies and vibrational frequencies obtained by the DFT calculations, which were used in the RRKM calculations. In particular, accuracy of those for TSs has not been well evaluated. These parameters are often adjusted to fit experimental rate data. In this work they were used without any adjustment. The approximations made can be one of the reasons. For the steady-state approximation to be valid, lifetimes of the intermediates should be very short compared to the reactants. This was fulfilled according to the present RRKM calculations. For example, the lifetime of **3i**, which was longest among the intermediates in the reactions of iodotoluene ions, was estimated to be 130 times shorter than **I2a** at 300 kJ mol^{-1}. Even though agreements between the theoretical and experimental rate-energy dependences were not perfect, they are satisfactory for the present purpose of kinetic analysis to get insight into the dissociation mechanisms.

3.2.3. Comparison with the other toluene ion derivatives

The reaction pathways of the isomeric halotoluene ions obtained here are similar to those of the isomeric ions of methylated toluene (ethylbenzene and xylene) [6] and chlorotoluene [17] reported previously. The present kinetic analysis predicts that Bz$^+$ is the major $C_7H_7^+$ product in the dissociation of all the halotoluene ions investigated near the thresholds. This agrees with most experimental results including those of product-resolved studies using ICR [9,11].

Although Bz$^+$ was found to be the major $C_7H_7^+$ product formed through rearrangements in all the dissociations of the *ortho*, *meta*, and *para* isomers of the chloro-, bromo-, and iodotoluene ions, the most significant pathways were not all the same. For the *m*- and *p*-halotoluene (X = Cl, Br, and I) and *o*-chlorotoluene ions, dissociations occurred mainly through the halogenated isotoluene intermediates with retaining the original positions of X and CH_3, whereas for the *o*-bromo- and *o*-iodotoluene ions, dissociations occurred mainly by isomerization to the alpha isomers. It should be noted that all the most significant pathways correspond to the MERPs needed to produce $C_7H_7^+$ from the molecular ions. The final steps of isomerizations from the molecular ions to the alpha isomers, **X2c** → **X1a** occur through a halogen shift. The barriers for the steps are listed in Table 1. For the halogen shift, the C–X bond should cleave first. It is well known that the bond energies increase in the order C–I < C–Br < C–Cl, being reflected in the barriers of steps, **X2c** → **X1a**. These or other steps to reach **X2c** are less energetically favored than the steps via the halogenated isotoluene ions in the dissociation of *m*- and *p*-halotoluene and *o*-chlorotoluene ions, whereas they are more favored in the dissociation of *o*-bromo- and *o*-iodotoluene ions.

Table 1 shows the calculated C–X bond energies of some isomeric substituted toluene ions. For the analogous molecular ions, the C–X bond energies increase in the order C–I < C–Br < C–Cl < C–CH_3 < C–H, which agrees with the general tendency. Tr$^+$ and Bz$^+$ are produced from the dissociation of toluene and ethylbenzene ions [2,3,5,6,20,23,28]. As shown in Table 1, the

Table 1
The calculated critical energies of some reactions of $C_7H_7X^{+\bullet}$ [a]

Reaction	X				
	I [b]	Br [c]	Cl [d]	CH_3 [e]	H [f]
X1a → Bz^+ + X•	45	57	112	154	224
X1a → Tr^+ + X•	173	155	125	131	207
X2c → **X1a** (via **X1a2c**)	32	39	58	–	–
X2a → oTl^+ + X•	211	237	318	354	381
X3a → mTl^+ + X•	223	247	326	366	387
X4a → pTl^+ + X•	243	268	348	385	395

[a] For the formation of Bz^+ and Tl^+, the values correspond to the C–X bond energies of the reactants. For the Tr^+ formation, the values are the barriers of the corresponding MERPs.
[b] This work. The B3LYP/6-311G(d,p)(C,H)/SDD(I) result.
[c] This work. The B3LYP/6-311G(d,p)(C,H)/SDD(Br) result.
[d] Ref. [36]. The B3LYP/6-311 + G(3df,2p)//B3LYP/6-31G(d) result.
[e] Ref. [6]. The B3LYP/6-311 + G(3df,2p)//B3LYP/6-31G(d) result.
[f] Ref. [5]. The G3//B3LYP result. Those for the Tl^+ formation were calculated in this work.

calculated critical energies for the formation of Tr^+ from the two molecular ions are smaller than those for Bz^+ formation. The former is favored at low energies, and the latter is favored at high energies, because the direct bond cleavage is entropically more favored with increasing energy. However, for α-halotoluene ions, the energies needed for Tr^+ formation are larger than those for the Bz^+ formation. This is because the former occurs through rearrangement steps, including the cleavages of C–H or C–C bonds, which require larger energies than those of C–X bonds. Since the formation of Tr^+ is less favored both entropically and energetically, it would not be observed in dissociation of the α-halotoluene ions. Similarly, considering the entropic effect, the formation of Tl^+ from the *o*-, *m*-, or *p*-halotoluene ions can dominate the Bz^+ formation at energies much higher than its threshold. In the dissociation of *o*-, *m*-, and *p*-iodotoluene ions, particularly the former two, the formation of Tl^+ can compete with Bz^+ formation at relatively low energies as described above.

4. Conclusions

The PESs for the dissociation and isomerization of bromo- and iodotoluene ions were obtained using B3LYP calculations. The RRKM model calculations were carried out to obtain the dissociation rate constants. For all the molecular ions, the only $C_7H_7^+$ product was Bz^+ in the dissociations occurring below the threshold for Tl^+ formation. From the α-isomers (**B1a** and **I1a**), Bz^+ was produced by direct C–X bond cleavage. In the reactions of **B3a**–**B4a** and **I3a**–**I4a**, the rearrangements to the halogenated isotoluene ions followed by C–X bond cleavage were the main dissociation mechanisms. The rearrangement to **B1a**, or **I1a**, of which the final step included an X shift, followed by C–X bond cleavage was more important in the dissociation of **B2a** or **I2a**. The interconversion among the *o*-, *m*-, and *p*-halotoluene ions contributed to the dissociations negligible. As increasing energy, the formation of Tl^+ became important because it is entropically more favored than the rearrangements. For the *o*- and *m*-iodotoluene ions, its contribution should be considered even in the slow dissociations occurring with $k \approx 10^5\ s^{-1}$.

Acknowledgements

This work was supported by the Korea Research Foundation Grant funded by the Korean Government (MOEHRD) (KRF-2007-313-C00351), in which the main calculations were performed using the supercomputing resource of the Korea Institute of Science and Technology Information (KISTI). The author wishes to thank Jin Hong Park and Sun Hwa Jung for their assistance in theoretical calculations.

References

[1] P.N. Rylander, S. Meyerson, H.M. Grubb, J. Chem. Phys. 79 (1957) 842.
[2] C. Lifshitz, Acc. Chem. Res. 27 (1994) 138.
[3] C. Lifshitz, Y. Gotkis, A. Ioffe, J. Laskin, S. Shaik, Int. J. Mass Spectrom. Ion Process. 125 (1993) 7.
[4] M.K.Z. Hoffman, Z. Naturforsch. 29a (1974) 1077.
[5] J.C. Choe, J. Phys. Chem. A 110 (2006) 7655.
[6] J.C. Choe, Chem. Phys. Lett. 435 (2007) 39.
[7] S. Olesik, T. Baer, J.C. Morrow, J.J. Ridal, J. Buschek, J.L. Holmes, Org. Mass Spectrom. 24 (1989) 1008.
[8] T. Baer, J.C. Morrow, J.D. Shao, S. Olesik, J. Am. Chem. Soc. 110 (1988) 5633.
[9] B. Kim, S.K. Shin, J. Chem. Phys. 106 (1997) 1411.
[10] B. Kim, S.K. Shin, J. Phys. Chem. A 106 (2002) 9918.
[11] S.K. Shin, B. Kim, R.L. Jarek, S.J. Han, Bull. Korean Chem. Soc. 23 (2002) 267.
[12] S.K. Shin, S.J. Han, B. Kim, Int. J. Mass Spectrom. Ion Process. 157 (1996) 345.
[13] C.Y. Lin, R.C. Dunbar, J. Phys. Chem. 98 (1994) 1369.
[14] R.C. Dunbar, J.P. Honovich, B. Asamoto, J. Phys. Chem. 92 (1988) 6935.
[15] Y.S. Cho, M.S. Kim, J.C. Choe, Int. J. Mass Spectrom. Ion Process. 145 (1995) 187.
[16] J.C. Choe, M.S. Kim, Int. J. Mass Spectrom. Ion Process. 107 (1991) 103.
[17] J.C. Choe, J. Phys. Chem. A 112 (2008) 6190.
[18] F.W. McLafferty, J. Winkler, J. Am. Chem. Soc. 96 (1974) 5182.
[19] F.W. McLafferty, F.M. Bockhoff, J. Am. Chem. Soc. 101 (1979) 1783.
[20] J.A.A. Jackson, S.G. Lias, P. Ausloos, J. Am. Chem. Soc. 99 (1977) 7515.
[21] J.C. Traeger, B.M. Kompe, Int. J. Mass Spectrom. Ion Process. 101 (1990) 111.
[22] C. Lifshitz, I. Levin, S. Kababia, R.C. Dunbar, J. Phys. Chem. 95 (1991) 1667.
[23] J.H. Moon, J.C. Choe, M.S. Kim, J. Phys. Chem. A 104 (2000) 458.
[24] W.G. Hwang, J.H. Moon, J.C. Choe, M.S. Kim, J. Phys. Chem. A 102 (1998) 7512.
[25] Y.H. Kim, J.C. Choe, M.S. Kim, J. Phys. Chem. A 105 (2001) 5751.
[26] J. Grotemeyer, H.F. Grützmacher, Current Topics in Mass Spectrometry and Chemical Kinetics, in A. Macoll (ed.). Heyden, London, 1982, p. 29.
[27] H.F. Grützmacher, N. Harting, Eur. J. Mass Spectrom. 9 (2003) 327.
[28] S. Schulze, A. Paul, K.-M. Weitzel, Int. J. Mass Spectrom. 252 (2006) 189.
[29] T.D. Fridgen, J. Troe, A.A. Viggiano, A.J. Midey, S. Williams, T.B. McMahon, J. Phys. Chem. A 108 (2004) 5600.
[30] M.J.S. Dewar, D. Landman, J. Am. Chem. Soc. 99 (1977) 2446.
[31] J.C. Choe, Rapid Commun. Mass Spectrom. 17 (2003) 207.
[32] J.C. Choe, Int. J. Mass Spectrom. 237 (2004) 1.
[33] J.C. Choe, Int. J. Mass Spectrom. 242 (2005) 5.
[34] D. Norberg, P.-E. Larsson, N. Salhi-Benachenhou, J. Phys. Chem. A 112 (2008) 4694.
[35] S.-J. Kim, C.-H. Shin, S.K. Shin, Mol. Phys. 105 (2007) 2541.
[36] J. Seo, H.-I. Seo, S.-J. Kim, S.K. Shin, J. Phys. Chem. A 112 (2008) 6877.
[37] T. Baer, W.L. Hase, Unimolecular Reaction Dynamics: Theory and Experiments, Oxford, New York, 1996.
[38] M.J. Frisch, G.W. Trucks, H.B. Schlegel, G.E. Scuseria, M.A. Robb, J.R. Cheeseman, J.A. Montgomery Jr, T. Vreven, K.N. Kudin, J.C. Burant, J.M. Millam, S.S. Iyengar, J. Tomasi, V. Barone, B. Mennucci, M. Cossi, G. Scalmani, N. Rega, G.A. Petersson, H. Nakatsuji, M. Hada, M. Ehara, K. Toyota, R. Fukuda, J. Hasegawa, M. Ishida, T. Nakajima, Y. Honda, O. Kitao, H. Nakai, M. Klene, X. Li, J.E. Knox, H.P. Hratchian, J.B. Cross, V. Bakken, C. Adamo, J. Jaramillo, R. Gomperts, R.E. Stratmann, O. Yazyev, A.J. Austin, R. Cammi, C. Pomelli, J.W. Ochterski, P.Y. Ayala, K. Morokuma, G.A. Voth, P. Salvador, J.J. Dannenberg, V.G. Zakrzewski, S. Dapprich, A.D. Daniels, M.C. Strain, O. Farkas, D.K. Malick, A.D. Rabuck, K. Raghavachari, J.B. Foresman, J.V. Ortiz, Q. Cui, A.G. Baboul, S. Clifford, J. Cioslowski, B.B. Stefanov, G. Liu, A. Liashenko, P. Piskorz, I. Komaromi, R.L. Martin, D.J. Fox, T. Keith, M.A. Al-Laham, C.Y. Peng, A. Nanayakkara, M. Challacombe, P.M.W. Gill, B. Johnson, W. Chen, M.W. Wong, C. Gonzalez, J.A. Pople, Gaussian 03, Revision C. 02. Gaussian, Inc., Wallingford CT, 2004.
[39] D. Andrae, U. Häußermann, M. Dolg, H. Stoll, H. Preuß, Theor. Chim. Acta 77 (1990) 123.
[40] T. Beyer, D.R. Swinehart, ACM Commun. 16 (1973) 379.
[41] A.C. Petersen, S. Hammerum, Int. J. Mass Spectrom. 210–211 (2001) 403.
[42] A. Nixdorf, H.-F. Grüzmacher, Int. J. Mass Spectrom. 219 (2002) 409.
[43] D. Kirchhoff, H.-F. Grüzmacher, H. Grüzmacher, Int. J. Mass Spectrom. 249–250 (2006) 130.
[44] Y.H. Yim, M.S. Kim, J. Phys. Chem. 97 (1993) 12122.
[45] S.H. Lim, J.C. Choe, M.S. Kim, J. Phys. Chem. A 102 (1998) 7375.